Review

Dimethylsulfoxide-quenched hydrogen/deuterium exchange method to study amyloid fibril structure

Masaru Hoshino [a,*], Hidenori Katou [b], Kei-ichi Yamaguchi [c], Yuji Goto [d]

[a] *Graduate School of Pharmaceutical Sciences, Kyoto University, 46-29 Yoshida-Shimoadachi, Sakyo-ku, Kyoto 606-8501, Japan*
[b] *Laboratory of Biochemistry, National Cancer Institute, NIH, Bethesda, MD 20892, USA*
[c] *Center for Emerging Infectious Diseases, Gifu University, Yanagido 1-1, Gifu 501-1194, Japan*
[d] *Institute for Protein Research, Osaka University and CREST, Japan Science and Technology Agency, Yamadaoka 3-2, Suita, Osaka 565-0871, Japan*

Abstract

A general method to analyze the structure of a supramolecular complex of amyloid fibrils at amino acid residue resolution has been developed. This method combines the NMR-detected hydrogen/deuterium (H/D) exchange technique to detect hydrogen-bonded amide groups and the ability of the aprotic organic solvent dimethylsulfoxide (DMSO) to dissolve amyloid fibrils into NMR-observable, monomeric components while suppressing the undesired H/D exchange reaction. Moreover, this method can be generally applied to amyloid fibrils to elucidate the distribution of hydrogen-bonded amino acid residues in the three-dimensional molecular organization in the amyloid fibrils. In this study, we describe theoretical considerations in the H/D exchange method to obtain the structural information of proteins, and the DMSO-quenched H/D exchange method to study a supramolecular complex of amyloid fibrils. A possible application of this method to study the interaction of a protein/peptide with phospholipid membrane is also discussed.
© 2007 Elsevier B.V. All rights reserved.

Keywords: Hydrogen/deuterium exchange; Amyloid fibril; Nuclear magnetic resonance; Protein structure; Hydrogen bond

Contents

* Corresponding author. Tel.: +81 75 753 4531; fax: +81 75 753 4529.
  E-mail address: hoshi@pharm.kyoto-u.ac.jp (M. Hoshino).

1. Introduction

An increasing number of proteins have been found to organize into unbranched, long fibrillar structures, called amyloid fibrils. The formation of these amyloid fibrils was first related to various serious diseases such as Alzheimer's disease; however, a variety of non-pathogenic proteins have also been found to form similar fibrillar structures. The observation that many proteins have the ability to form similar fibrillar structures with common features suggests that this is a general characteristic of polypeptide chains. Considerable efforts have been made to obtain structural information of the amyloid fibrils using various techniques including X-ray diffraction, electron microscopy, and solid-state NMR, and it is now considered that amyloid fibrils are composed predominantly of β-sheet structures, where the β-strands are arranged perpendicular to the fibrillar axis, into so-called cross-β structure. In addition, recent studies on fibrous microcrystals formed by peptides with either seven or twelve residues have confirmed the structural details of the cross-β spine of fibrils [1,2]. However, the nature of amyloid fibrils as non-crystalline, insoluble, and large molecular assemblies, makes it difficult to access them by established structural techniques such as X-ray crystallography or high-resolution solution NMR. We recently developed a novel method to obtain the structural and dynamic properties of amyloid fibrils in an aqueous environment using solution NMR spectroscopy in combination with hydrogen/deuterium (H/D) exchange [3,4]. This method makes it possible to probe the structured region of the protein molecule organized into the amyloid fibrils at residue resolution. Moreover, it can be generally applied to all amyloid fibrils, and is potentially applicable to other structurally difficult targets such as membrane interacting proteins.

The H/D exchange method combined with high-resolution NMR spectroscopy provides detailed picture of the structure and thermodynamic stability of proteins at residue resolution. This method has been widely applied not only to the native structures but also to various conformational states of proteins, such as chemically or physically denatured states, and equilibrium or kinetic folding intermediates, in which direct determination of the three-dimensional structure is not possible [5–8]. However, this technique inherently has a serious limitation on the apparent molecular mass of the target protein (complex) as it monitors the exchange kinetics using solution NMR, in which signal height is approximately inversely proportional to the molecular weight of the object. The amyloid fibril is a supramolecular assembly composed of numerous protein molecules, and therefore, direct application of the H/D exchange method is difficult. Although the amyloid fibril is generally very stable under the aqueous conditions where it forms, we found that it dissolved (decomposed) into monomeric protein molecules at high concentration of several organic solvents [9]. Furthermore, the presence of an extremely high (>90%) concentration of aprotic organic solvent DMSO resulted in significant deceleration of the H/D exchange reaction. Because of these properties, it is possible to follow the exchange kinetics of the amyloid fibrils by dissolving the fibrils in DMSO and acquiring two-dimensional NMR spectra. Similar method was also independently developed by Alexandrescu [10], and it was also demonstrated to provide a quantitative measure of a protection factor of each amide site in the amyloid fibril [11]. In this study, we describe the theoretical background of the DMSO-quenched H/D exchange method, and recent applications to determine the organization of protein molecules in the amyloid fibrils.

2. Basic theory of H/D exchange in protein

2.1. Intrinsic rate constant and protection factor

Hydrogen atoms in backbone amide groups of unstructured small peptides are labile and exchange easily with those of the solvent molecules. The exchange reaction is catalyzed by both acids and bases, and its rate is highly dependent on the pH of the solution. The intrinsic exchange rate constant of hydrogen in a freely exposed amide group is described as

$$k_{int} = k_w + k_{acid}[H^+] + k_{base}[OH^-] \qquad (1)$$

where k_{int}, k_w, k_{acid}, and k_{base} are the observed rate constant for exchange, the spontaneous rate constant in water, the acid catalyzed second-order rate constant, and the base catalyzed second-order rate constant, respectively. The dependence of the k_{int} value of amino acid residues on pH typically shows a V-shaped curve with minimum value at pH ∼3 under aqueous conditions (Fig. 1A). Changing the pH of the solution from the minimum value by one unit results in an increase in the rate by one order of magnitude. The exchange rate of a particular amide group can be sterically blocked by neighboring bulky side chains or induced by neighboring polar side chains; therefore, the exchange rate varies with the amino acid sequence. These inductive and steric blocking effects by the side chains of nearest-neighbor amino acid residues on each kinetic term have been quantified and tabulated as a function of temperature and pH [12]. Using these values, the k_{int} values of each individual amino acid residue in a particular sequence can be calculated. Intrinsic rate constants of amino acid residues in a protein sequence are significantly different from each other, ranging one order of magnitude between residues.

In a folded protein, the exchange rates of amide hydrogen in a stable element of the secondary or tertiary structure are further
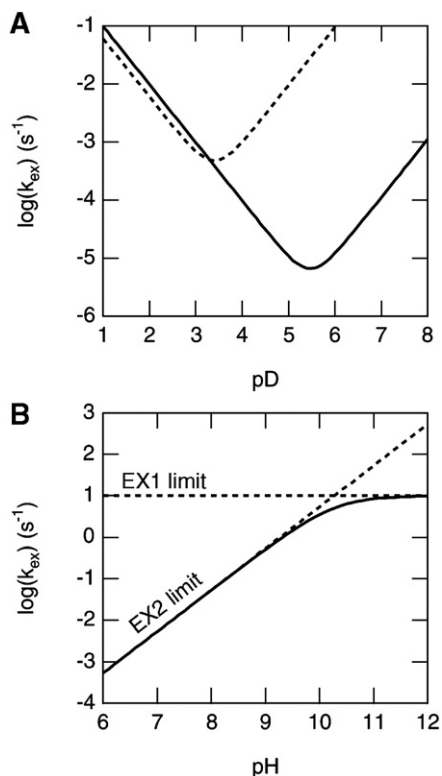
Fig. 1. (A) pH dependence of the H/D exchange rate constant in 95% DMSO/5% D_2O (solid line) and 100% D_2O (dashed line). Simulation was performed according to Eq. (1) in Zhang et al. using the following parameters: $pH_{min}=5.47$, $k_{min}=6.54\times10^{-6} s^{-1}$, $pH_{min}=3.40$, and $k_{min}=4.72\times10^{-4} s^{-1}$. (B) pH dependence of the H/D exchange rate of proteins under the EX1 and EX2 conditions, simulated by Eqs. (1) and (3) using the following parameters: $k_c=2.0\times10^4 s^{-1}$, $k_o=10 s^{-1}$, $k_{acid}=0.69 M^{-1} s^{-1}$, $k_{base}=1.9\times10^8 M^{-1} s^{-1}$, and $k_w=5.3\times10^{-4} s^{-1}$.

retarded by the formation of hydrogen bonds with carbonyl or hydroxyl groups in other residues or by being buried in the hydrophobic core of the protein. The retardation of the exchange rate observed in the folded protein is directly related to higher order structures. The ratio between observed exchange rate and the intrinsic exchange rate, which is expected if that site is freely exposed, is called the protection factor and is defined by

$$P = k_{int}/k_{ex} \tag{2}$$

where k_{int} is the intrinsic rate constant of hydrogen under the reaction conditions (calculated as a function of amino acid sequence, pH, and temperature), and k_{ex} is the observed value for the exchange rate in the protein.

While we are interested in the structural stability of the protein at each amino acid residue, the intrinsic exchange rate itself can vary by one order of magnitude depending on the local amino sequence. That is, the observed exchange rate depends both on the structural term defined by the stability of the protein and the effect of the local amino acid sequence that should be removed. The conversion of the obtained exchange rate to the protection factor serves as the elimination of the sequence dependence and provides thermodynamic stability of that site only if the exchange conditions are well approximated by the

EX2 regime (see below). The protection from the exchange is often very high and typically 10^4 to 10^6 or more in the native structure of the globular proteins.

2.2. Exchange mechanisms

For a hydrogen exchange reaction to occur in an amide group, which forms a stable hydrogen bond and/or is buried inside the protein core, such hydrogen must become an exchange competent state either by small-scale structural fluctuations, termed local unfolding or breathing, or by transient but complete unfolding (global unfolding) of the whole molecule [13,14]. In either case, the exchange reaction at a particular amide in the folded protein is described as

$$NH_c \underset{k_c}{\overset{k_o}{\rightleftharpoons}} NH_o \xrightarrow{k_{int}} ND \tag{Scheme 1}$$
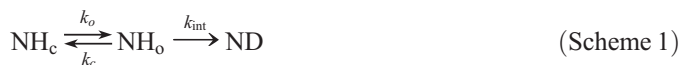
where NH_c and NH_o represent the amide groups either in the locally "closed" and "open" conformations or in the globally folded and unfolded molecules, respectively; ND is the exchanged amides; k_o and k_c are opening (unfolding) and closing (folding) rate constants, respectively; and k_{int} is an intrinsic exchange rate constant in a freely exposed, unprotected state. In the present scheme, backward exchange from ND to NH_o is neglected based on the assumption that the solvent D_2O is in excess as compared with the protein concentration.

Under steady-state conditions, the exchange rate constant (k_{ex}) of amide hydrogen in the reaction Scheme (1) is given by

$$k_{ex} = \frac{k_o k_{int}}{k_o + k_c + k_{int}} \tag{3}$$

Under the conditions where most of the H/D exchange experiments are performed, the folded conformation is favored over the unfolded form, so that $k_c \gg k_o$. Therefore, Eq. (3) can be approximated as

$$k_{ex} = \frac{k_o k_{int}}{k_c + k_{int}} \tag{4}$$

Eq. (4) has two extreme limits. When $k_c \gg k_{int}$, which is generally expected at low pH and temperature, the exchange rate becomes

$$k_{ex} = \frac{k_o k_{int}}{k_c} = K_o k_{int} \tag{5}$$

where $K_o = k_o/k_c$ is the equilibrium constant between open and closed conformations. This situation is termed the EX2 (bimolecular exchange) limit. Under EX2 conditions, the H/D exchange rate expressed by the protection factor P gives the thermodynamic stability of that site as

$$\Delta G_{ex} = -RT\ln K_o = -RT\ln\frac{k_{ex}}{k_{int}} = RT\ln P \tag{6}$$

where ΔG_{ex} is the Gibb's free energy of unfolding (opening) of that amide site, R is the gas constant, and T is absolute temperature.

The other extreme limit, termed as the EX1 (monomolecular exchange) limit, is usually fulfilled at high pH and temperature, where $k_c << k_{int}$. In this extreme limit, the exchange reaction is rate limited by the opening event of the amide site, and Eq. (4) reduces to

$$k_{ex} = k_o \tag{7}$$

Under EX1 conditions, the exchange rate constant gives the kinetic constant of the opening (unfolding) reaction. In this case, conversion of exchange rates to protection factors is almost meaningless although it is mathematically valid.

The obtained experimental value of the exchange rate should be correctly analyzed depending on limiting conditions that can be satisfied. From the pH dependence of the exchange rate, it is possible to determine whether the exchange reaction of interest is governed by the EX1 or EX2 limit. Under the EX2 limit, the exchange rate is proportional to the intrinsic exchange rate given by Eq. (1), and it depends dramatically on the pH of the solution. On the other hand, the observed exchange rate is almost pH-independent under the EX1 conditions (Fig. 1B).

2.3. Exchange reaction in very high concentrations of DMSO

Zhang et al. [15] carefully examined the H/D exchange rate constant of a peptide-based model compound in DMSO. They found that the exchange rate decreased by about 100 times in the presence of as much as 90–95% of DMSO as compared with that in aqueous conditions. In addition, the pH dependence of the rate constant was different from that in aqueous conditions, and the pH at which the exchange rate goes through a minimum was shifted from ∼3 in water to ∼5 in 95% DMSO (Fig. 1A). As described above, the H/D exchange reaction is catalyzed by both acids and bases (Eq. (1)). Zhang et al. [15] explained the reason for this dramatic deceleration and shift of the minimal value of pH for the exchange rate. They discussed that the transient formation of deprotonated amide that is necessary for the base-catalyzed exchange reaction becomes unfavorable in the presence of a high concentration of organic solvent such as DMSO.

$$NH + D_2O \rightleftharpoons [NH \cdots OD^- + D^+ \rightleftharpoons N \cdots HOD + D^+]$$
$$\rightleftharpoons ND + HOD \tag{Scheme 2}$$
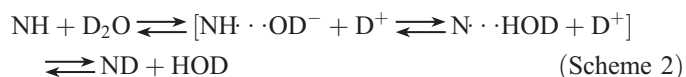
Generally, a very high concentration of organic solvent such as DMSO is unfavorable for charged states. This also appears as a dramatic increase in the pK_a value of acid. For example, the pK_a value of acetate, which is 4.76, becomes as much as 12.6 in 100% DMSO. As a result, the appropriate acid and base combination to control pH is completely different in DMSO from that ordinarily used in aqueous solvents. As described by Zhang et al. [15], dichloroacetic acid, which is a relatively strong acid with a pK_a value of 1.48 in water, becomes a weak acid with a pK_a value of 6.4 in 100% DMSO. Therefore, it acts as an appropriate buffer in very high concentrations of DMSO to keep the pH of the solution around 5, where the exchange rate is minimum.

3. Experimental scheme

3.1. Rapid dissolution of amyloid fibrils by DMSO

In the case of a water-soluble protein with <30 kDa molecular mass, H/D exchange experiments are relatively straightforward to perform, by dissolving protein into deuterated buffer and measuring appropriate NMR spectra successively. The cross-peak intensity in the spectra that detect amide protons, such as ^1H–^{15}N heteronuclear single quantum correlation (HSQC) or the fingerprint (H^N–H^α cross-peak) region of ^1H–^1H total correlation spectroscopy (TOCSY), is linearly proportional to the occupancy of ^1H in that amide group. Therefore, progress of the H/D exchange reaction can be observed as a decrease in peak intensity in the spectrum, and a plot of peak intensity as a function of exchange time results in a single exponential decay, which is given by

$$I(t) = I(0)\exp(-k_{ex}t) \tag{8}$$

where t is the exchange time, $I(0)$ and $I(t)$ are peak intensity at time zero and time t, respectively, and k_{ex} is the exchange rate constant.

The line width of the NMR signal is significantly broadened with the increase in rotational correlation time of the object, which is approximately proportional to its molecular weight. Therefore, direct measurement of NMR spectra of huge macromolecular complexes such as amyloid fibrils is practically impossible because the signal width is infinitely broadened. To overcome this problem, we recently developed a novel method to monitor the H/D exchange reaction in huge macromolecular complexes such as amyloid fibrils. This method takes advantage of the unique character of DMSO to dissolve (decompose) amyloid fibrils into monomeric protein molecules. Hirota-Nakaoka et al. [9] investigated the dissolving effect of several organic solvents such as TFE, HFIP, and DMSO. Among them, they found that only DMSO completely dissolved amyloid fibrils formed by β2-microglobulin (β2-m). Fig. 2 shows the dissolving effect of high concentrations of DMSO on preformed amyloid fibrils of β2-m evidenced by electron micrographs and light scattering. Because of the large molecular weight of amyloid fibrils, the scattering intensity was much larger as compared with that of the monomeric form of the protein. However, the scattering intensity of amyloid fibrils transferred into 80% (v/v) DMSO decreased to the same level as that of the monomeric protein. This suggests that a high concentration of DMSO can dissolve amyloid fibrils of β2-m very quickly into their monomeric components within the dead time of NMR measurement. Similar results were obtained for amyloid fibrils of Aβ(1–40) peptides (MH and YG, unpublished results), indicating the general feature of DMSO to dissolve amyloid fibrils composed of various proteins. Although the exact oligomeric state of the molecules in 95% (v/v) DMSO is not known, and dimeric or higher oligomeric states may still be present, there was no difference in line width in the NMR spectra recorded with samples prepared from monomeric protein and preformed amyloid fibrils.
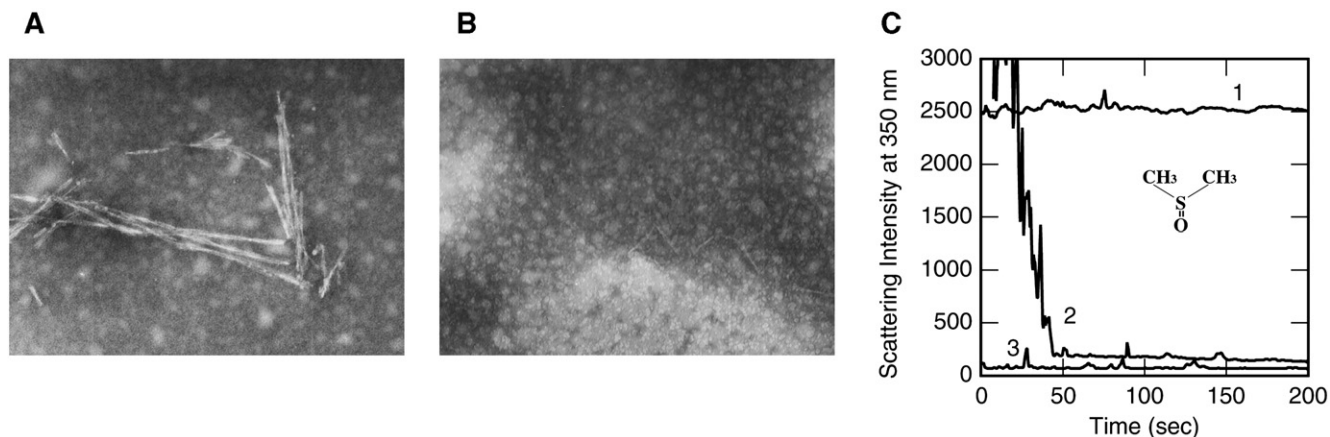
Fig. 2. Dissolving effect of DMSO on amyloid fibrils formed by β2-m. Electron micrograph of amyloid fibrils dissolved in (A) 20 mM HCl and (B) 80% DMSO and 20 mM HCl. (C) Light scattering of amyloid fibrils at 350 nm when added to (1) 20 mM HCl and (2) 80% DMSO and 20 mM HCl. Line (3) shows light scattering of monomeric β2-m in water. The chemical structure of DMSO is also shown. Data were taken from Hirota-Nakaoka et al. [9] with permission.

Another important feature of DMSO is that it has no labile hydrogen atoms that potentially exchange with amide hydrogen of proteins. In addition, when present in a very high concentration, it effectively reduces the base-catalyzed H/D exchange reaction. This results in the deceleration of the H/D exchange reaction by ∼100 times as compared with that in aqueous solvent [15]. Taking advantage of these unique features of DMSO to rapidly dissolve amyloid fibrils and quench the H/D exchange reaction, we designed an experimental method that allowed monitoring the H/D exchange reaction of each protein molecule in the amyloid fibrils at residue resolution [3,4]. The process is described as follows: (1) Prepare amyloid fibrils under the usual aqueous conditions. (2) Transfer the fibrils into deuterated buffer to perform the H/D exchange reaction. (3) After incubating for various exchange times, lyophilize the sample to remove deuterated aqueous buffer. (4) Dissolve the lyophilized amyloid fibrils at high (>95%) concentrations of DMSO at appropriately adjusted pH value. (5) Record 2D NMR spectra successively to detect resonance signals from exchange-protected residues. Although protein molecules are highly denatured in the presence of high concentrations of DMSO, and each residue in the protein is thus expected to exchange with the solvent at its intrinsic exchange rate, the use of a high concentration of DMSO reduces the exchange rate sufficiently to record several HSQC spectra (Fig. 3A). It is noted that a similar approach using DMSO and NMR was independently developed by Alexandrescu [10].

3.2. Minimizing the effect of backward exchange

The basic idea of the DMSO-quenched H/D exchange method described above is that the H/D exchange rate can be significantly slowed down in the presence of a very high concentration of DMSO, which has no exchangeable hydrogen. Ideally, if a partially deuterated protein sample, which has been subjected to H/D exchange under aqueous conditions, is dissolved in 100% DMSO, further exchange in this pure

organic solvent would be completely "frozen." In practice, however, this does not work for the following reasons. First, it is very difficult to avoid any contamination of water molecules in DMSO, as it is a highly hygroscopic solvent. Second, it is not possible to strictly control the pH of the sample, which is necessary to keep the intrinsic exchange rate to a minimum. Third, even if it is possible to remove any contamination of water in DMSO, undesired exchange reactions from one amide site to another may occur. This possible "flip-flop" between amide hydrogen could severely disturb the obtained experimental results.

Because the total amount of water molecules is very low in the DMSO-quenched H/D exchange method, it is very sensitive to contamination by H_2O. Therefore, H_2O contamination should be avoided as much as possible when performing the experiment. To minimize the effect of water contamination, we decided to use a mixture of 95% (v/v) DMSO-d6 and 5% (v/v) D_2O at pD 5 adjusted by dichloroacetate-d2 titrated with NaOD as a quenching buffer for the H/D exchange. The quenching buffer contains 5% (v/v) of D_2O, and therefore, residual exchange reaction occurs in it. However, this residual exchange by 5% (v/v) D_2O is not a serious problem because any effect of residual exchange can be removed if the rate of the exchange reaction and contamination by H_2O is sufficiently small, as described below. In contrast, contamination by H_2O in the quenching buffer causes much more serious problems.

If we measure the 2D-NMR spectrum in the quenching buffer (95% (v/v) DMSO/5% (v/v) D_2O, pD 5), the intensity of each resonance peak decays exponentially at an intrinsic rate under those conditions (Fig. 3A). In an ideal case without any H_2O contamination in quenching buffer, however, any effects of exchange during the measurement of NMR spectra can be eliminated simply by taking the ratio of peak intensity between "reference" and "partially exchanged" sample. While the "reference" sample is not subjected to the H/D exchange reaction, the "partially exchanged" sample is incubated in aqueous deuterated buffer for a desired period in the form of
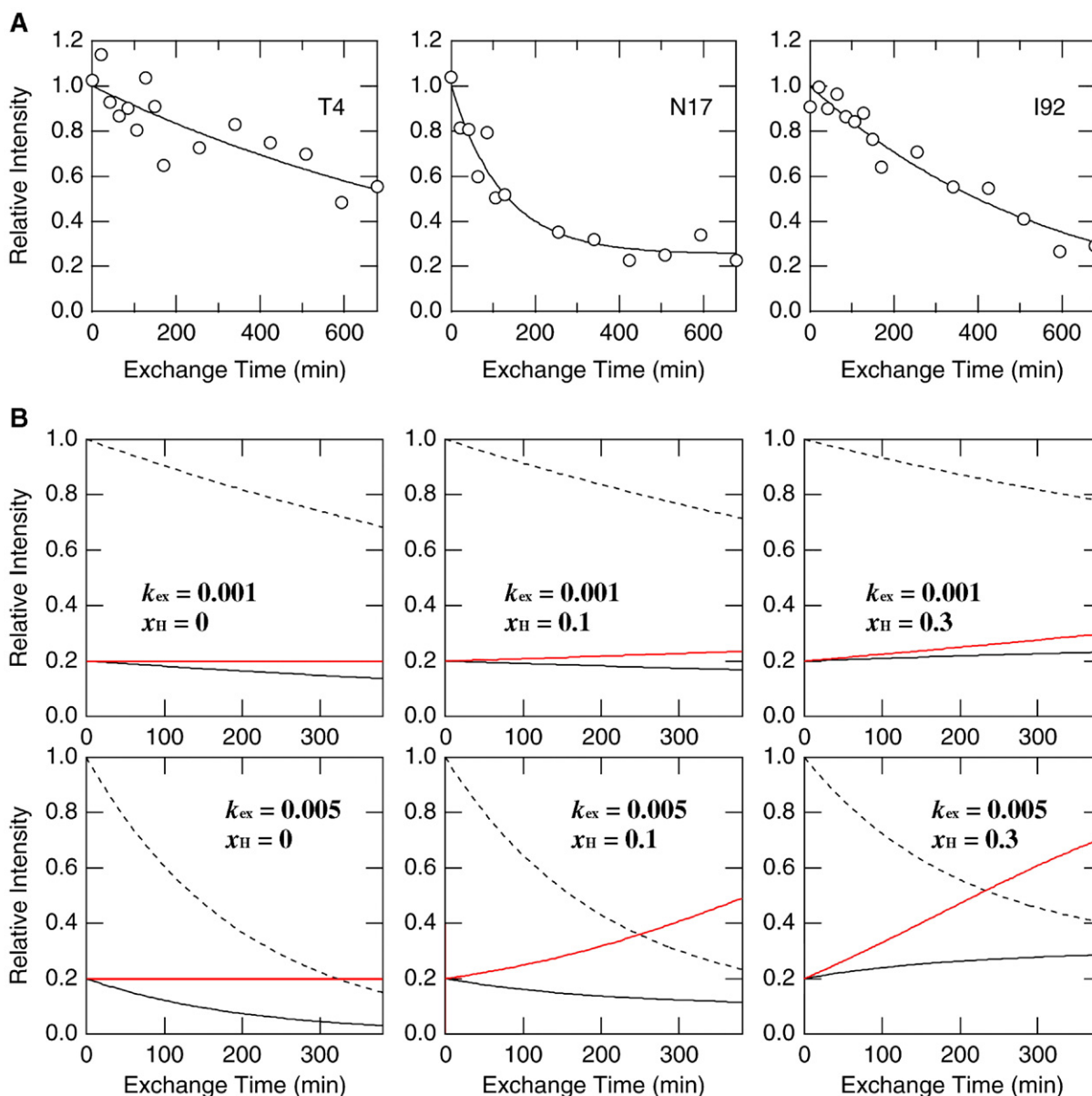
Fig. 3. H/D exchange reaction in DMSO-quenching buffer (95% DMSO–d6/5% D$_2$O, pD 5). (A) Experimental exchange kinetics of representative residues of β2-m at 25 °C. Circles indicate the peak intensities of successively measured ^{1}H–^{15}N HSQC spectra after dissolving protein in DMSO-quenching buffer. Solid line shows the curves fitted to single exponential functions. (B) Simulated H/D exchange kinetics in the "reference" and "exchanged" spectra. While broken line shows the signal decay of the "reference" spectra starting with the value of 1, black solid line indicates the decay of the "exchanged" spectra that starts at 0.2. The red line represents the ratio between "exchanged" and "reference" sample, showing strong dependence on both k_{ex} and x_H.

amyloid fibrils. The signal decay in each spectrum during the measurement is

$$I_{ref}(\tau_{DMSO}) = I_{ref}(0)\exp(-k_{ex}\ \tau_{DMSO}) \tag{9}$$

$$I_{ex}(\tau_{DMSO}) = I_{ex}(0)\exp(-k_{ex}\tau_{DMSO}) \tag{10}$$

where I_{ref} and I_{ex} are the peak intensities in the spectra of reference and partially H/D exchanged samples, respectively, as functions of the acquisition time, τ_{DMSO}, and k_{ex} is an exchange rate constant in the quenched buffer. The ratio of peak intensities between reference and partially exchanged spectra is

$$\text{ratio} = I_{ex}(\tau_{DMSO})/I_{ref}(\tau_{DMSO}) = I_{ex}(0)/I_{ref}(0) \tag{11}$$

Therefore, if both spectra were measured for the same acquisition time, any exchange reaction in the quenching buffer may be eliminated.

However, in the presence of any contamination by H$_2$O in the quenching buffer, the effect of the exchange reaction cannot be cancelled even by taking the ratio. Consider the exchange reaction between protonated and deuterated amide groups in

DMSO-quenching buffer, on the assumption that water molecules are in great excess as compared with protein concentration,

$$NH \underset{k_H}{\overset{k_D}{\rightleftharpoons}} ND \qquad (Scheme\ 3)$$

where NH and ND represent protonated and deuterated amide groups, respectively, and k_D and k_H are the rate constants for the deuteration and protonation of the amide, respectively. According to Scheme (3), the exchange rate constant of the reaction is defined by

$$k_{ex} = k_H + k_D \qquad (12)$$

and the time dependence of the protonated site is expressed as

$$\frac{d[NH]}{dt} = -k_D[NH] + k_H[ND] \qquad (13)$$

This derivative equation can be solved as

$$[NH] = \frac{k_H([NH]_0 + [ND]_0 + (k_D[NH]_0 - k_H[ND]_0)\exp(-k_{ex}t)}{k_{ex}} \qquad (14)$$

Now, we define the ratio of contaminated H_2O in the quenching buffer, x_H ($0 \leq x_H \leq 1$) as

$$X_H = \frac{[H_2O]}{[H_2O] + [D_2O]} \qquad (15)$$

Because k_D and k_H are linearly dependent on the concentrations of D_2O and H_2O, respectively, and from Eqs. (12) and (15), we obtain

$$k_D = (1 - x_H)k_{ex} \qquad (16)$$

$$k_H = x_H\ k_{ex} \qquad (17)$$

If we consider Eq. (14) as a signal decay in the partially exchanged sample in DMSO-quenching buffer, the following conditions are satisfied: $I_{ref}(0) = [NH]_0 + [ND]_0$, $I_{ex}(0) = [NH]_0$, and $I_{ex}(\tau_{DMSO}) = [NH]$. Here, coefficients are omitted for clarity. By substituting these equalities into Eq. (14), we obtain

$$I_{ex}(\tau_{DMSO}) = I_{ref}(0)\left[x_H + \left\{\frac{I_{ex}(0)}{I_{ref}(0)} - x_H\right\}\exp(-k\tau_{DMSO})\right] \qquad (18)$$

and also

$$I_{ref}(\tau_{DMSO}) = I_{ref}(0)\{x_H + (1 - x_H)\exp(-k\tau_{DMSO})\} \qquad (19)$$

If x_H is equal to zero, Eqs. (18) and (19) become the same as Eqs. (10) and (9), respectively. Eq. (19) predicts that the contamination of H_2O at a ratio of x_H resulted in the scaling down of the amplitude of the kinetic trace by $(1 - x_H)$ with an offset value of x_H. In contrast, the kinetic trace represented by Eq. (18) is rather complicated. Fig. 3B shows the simulation of kinetic traces using Eqs. (18) and (19) at several different values of k_{ex} and x_H in the case of $I_{ex}(0) = 0.2$. Apparent from the

simulation, the calculated value of the ratio between $I_{ex}(\tau_{DMSO})$ and $I_{ref}(\tau_{DMSO})$ depends considerably on both k_{ex} and x_H. If water contamination was ideally avoided, the ratio $I_{ex}(\tau_{DMSO})/I_{ref}(\tau_{DMSO})$ is independent of time as predicted by Eq. (11), resulting in a flat line at the value of 0.2. In contrast, if x_H and k_{ex} are significantly large, the ratio between exchanged and reference spectra increases rapidly to a value that is far from the expected value, $I_{ex}(0)/I_{ref}(0)$. Therefore, it is important to keep water contamination as low as possible, and to measure NMR spectra as quickly as possible.

From successive measurement of $^1H-^{15}N$ HSQC spectra of fully protonated ^{15}N-labeled β2-m in DMSO-quenching buffer, contamination by H_2O, x_H, is expected to be less than 0.3 and the exchange rate constants k_{ex} are ~ 0.002 min^{-1} for most residues (Fig. 3A). If all the measurements were finished within 100 min including the dead time for sample preparation, the effect of the exchange reaction occurring in DMSO-quenching buffer can be well eliminated by taking the ratio between partially exchanged spectra and reference spectra.

The more direct and complete method to eliminate any effects from contaminated water molecules is the two-step exponential fit. If it is possible to collect several NMR spectra with enough signal-to-noise ratio during the time course of the exchange in DMSO-quenching buffer, the peak intensities in these spectra can be fitted to the single exponential function (Eqs. (18) and (19)) to obtain the values of $I_{ex}(0)$ and $I_{ref}(0)$ directly. Even in this case, the water contamination and exchange rate should be kept as low as possible, otherwise the reliability of the fitted value of $I(0)$ may become very poor.

4. Application of the DMSO-quenched H/D exchange method to study amyloid fibrils

4.1. β2-microglobulin

β$_2$-Microglobulin (β2-m) normally functions as a light chain of the class I major histocompatibility complex on the cell surface, which, in a complex with the heavy chain, presents antigen to T-cells [16]. It is also identified as a major structural component of amyloid fibrils, which are deposited in patients receiving long-term hemodialysis for more than 10 years, and cause dialysis-related amyloidosis [17]. Although a 50-fold increase in the concentration of β2-m in blood during long-term hemodialysis is the most important risk factor for fibril formation, the exact mechanism by which β2-m is converted into stable amyloid fibrils is unknown. From *in vitro* studies, various methods that destabilize the native structure of β2-m have been shown to lead to the formation of amyloid fibrils [18–22]. Among them, it has been established that β2-m forms typical amyloid fibrils at acidic pH 2.5 in the presence of seeds, which are fragmented fibrils originally taken from patients [23,24].

According to the experimental scheme described above, we analyzed the structure and dynamics of amyloid fibrils formed by β2-m at pD 2.5. As a result, many amide peaks exhibited strong intensity even after incubation for 8 days, while several peaks showed considerable decreases in intensity (Fig. 4A).

Both spectra were measured for the same acquisition time with the same dead time in DMSO-quenching buffer. Therefore, the residues present in the "reference" spectrum but absent in the "exchanged" spectrum are indicated to be exchanged with solvent D_2O during the incubation time in deuterated aqueous buffer where protein molecules have been organized into amyloid fibrils. When the degree of exchange calculated as the ratio of peak intensities between exchanged and reference
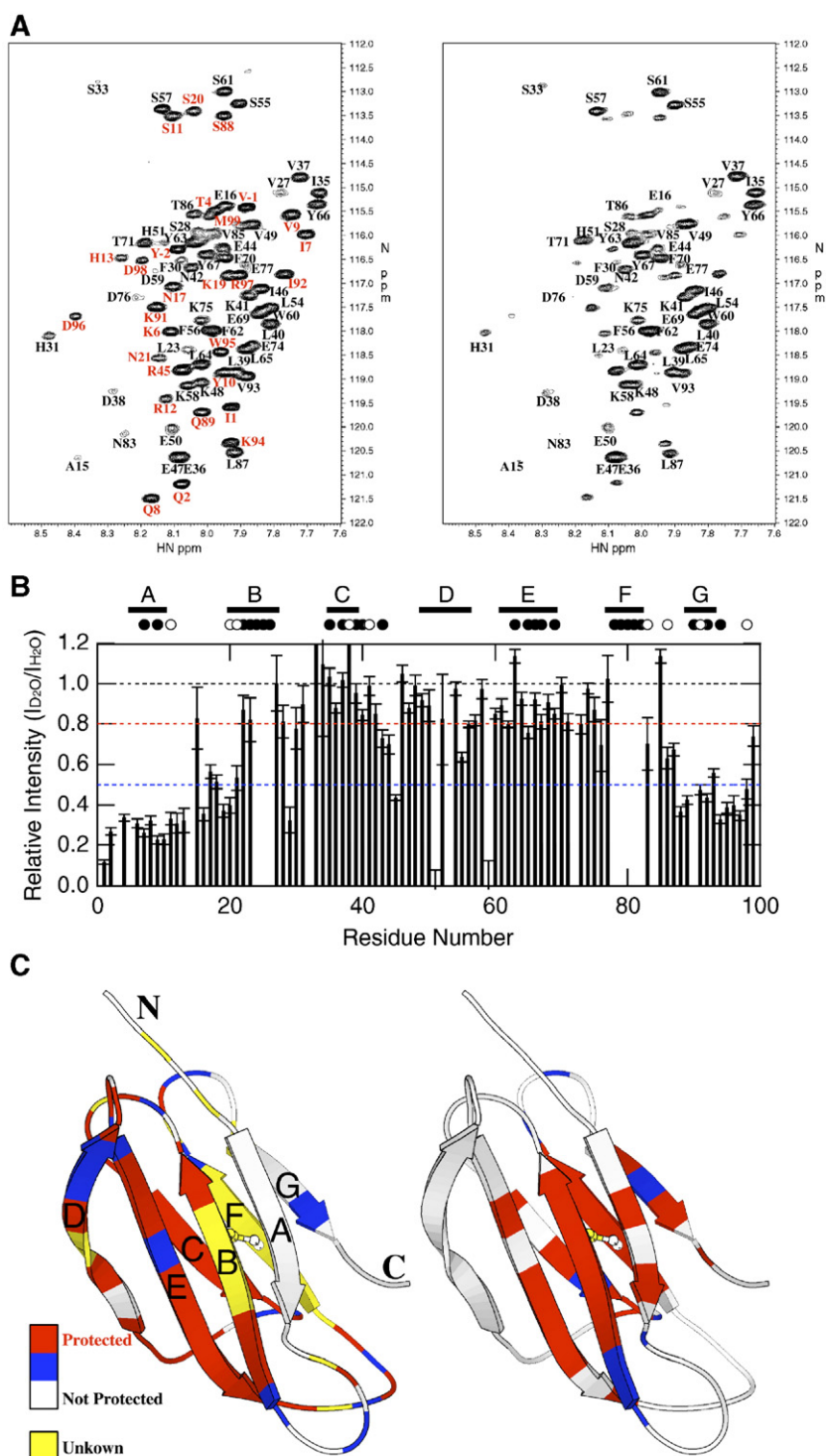

Fig. 4. (A) ^1H–^{15}N HSQC spectra of β2-m amyloid fibrils dissolved in DMSO-d6 at 25 °C. Reference spectrum of β2-m amyloid fibrils not subjected to H/D exchange (left), and partially exchanged spectrum that underwent exchange for 8 days at pD 2.5 and 25 °C. In the left panel, black and red labels represent the residues highly protected from and susceptible to exchange, respectively. (B) Relative peak intensity in the exchanged spectrum to that in the reference spectrum. The bars labeled A–G indicate the secondary structures in the native state. Red and blue dotted lines indicate the values used to classify the strongly and weakly protected residues, respectively. Black and white circles are the strongly and weakly protected residues, respectively, in the native structure of β2-m. (C) Comparison of the protected residues in the amyloid fibrils (left) and the native state (right) mapped on the three-dimensional native structure. Figures were taken from Hoshino [3] with permission.

spectra was plotted against residue number, most residues in the middle region of the molecule, even in the loop regions in the native form, were strongly protected from the H/D exchange (Fig. 4B). In contrast, the protection of the residues in both termini, especially in the N-terminus, was significantly weaker than in the middle part of the molecule, showing a characteristic trapezoidal shape with a relatively flat part in the middle of the sequence and slopes decreasing in intensity at both the N- and C-termini. The pattern of the protected residues was in contrast to that in the native state, in which only the seven β-stands (βA to βG) are protected, representing the β-barrel core of the immunoglobulin fold (circles in Fig. 4B, C). These results indicate that the amyloid fibril is stabilized by the extensive hydrogen-bond network that expands throughout the molecule

including the residues not involved in any secondary structures in the native structure.

It is known that β2-m forms two morphologically different amyloid fibrils under acidic conditions [23,25–28]. In the presence of seeds, β2-m forms "mature fibrils" with straight shape observed by electron microscopy (Fig. 5A). On the other hand, in the presence of high salt concentrations (200 mM), it spontaneously forms thinner fibrils with curved shape, sometimes called "immature fibrils" (Fig. 5B). The H/D exchange kinetics of these two morphologically different amyloid fibrils composed of the same amino acid sequence were compared by DMSO-quenched H/D exchange. The plot of the ratio of peak intensities between exchanged and reference spectra at different H/D exchange times against residue number clearly indicate the
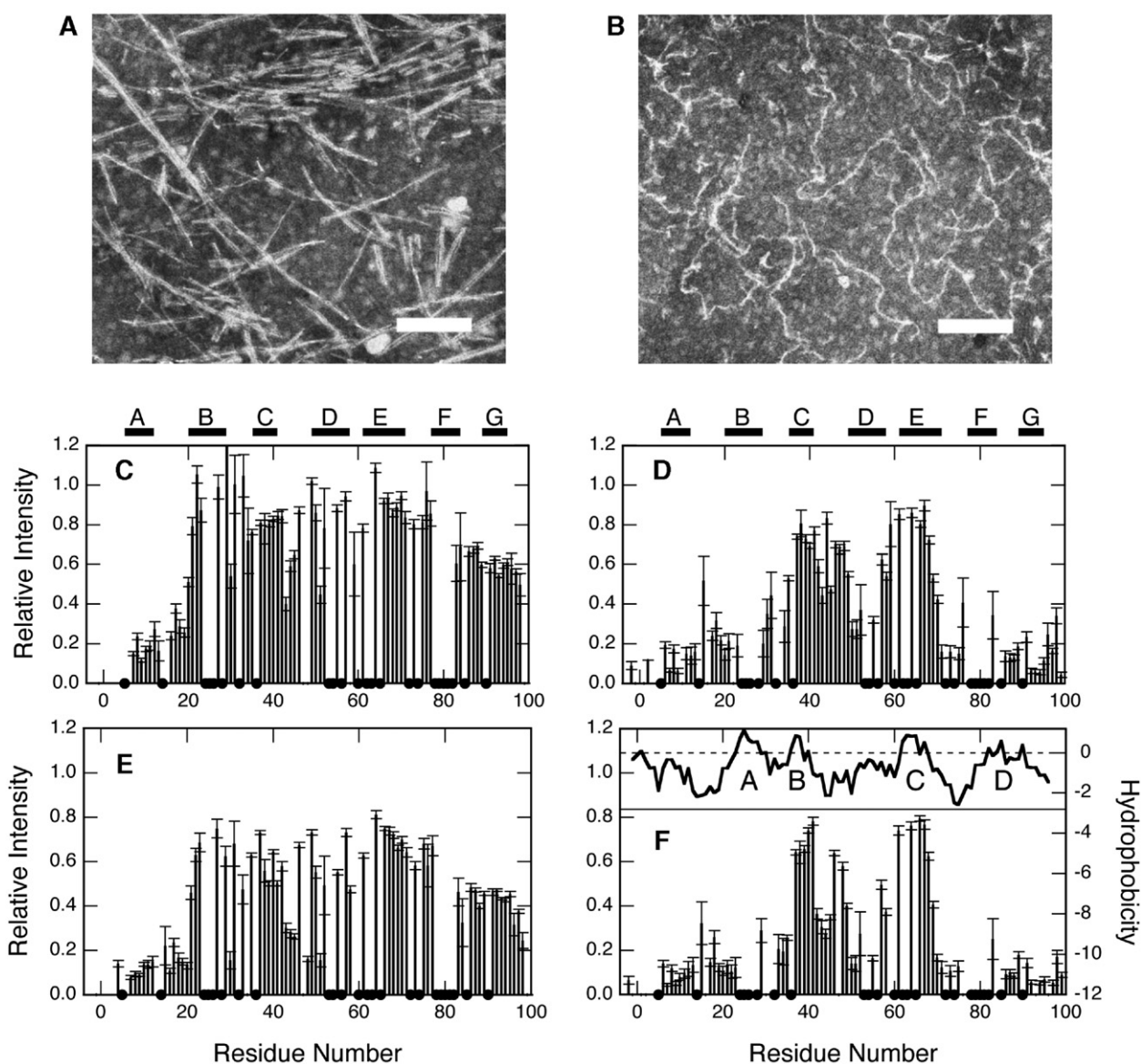

Fig. 5. Comparison between mature and immature fibrils formed by β2-m. Electron micrographs of (A) mature fibrils and (B) immature fibrils. The scale bar represents 200 nm. H/D exchange kinetics of mature fibrils at exchange times of (C) 14 h and (E) 206 h and of immature fibrils at exchange times of (D) 11.5 h and (F) 204 h. The residues for which data were not available are indicated by filled circles. The hydropathy profile of β2-m calculated using the scale described by Kyte and Doolittle [41] averaged over a sliding window of seven residues is shown in (F). The positions of four major hydrophobic sites are designated A to D in (F). The locations of secondary structures in the native structure are indicated at the top of the figure. The figure was taken from Yamguchi et al. [4] with permission.

difference between mature fibrils and immature filaments (Fig. 5C–F). In mature fibrils, most residues with the exception of 20 residues from the N-terminus were significantly protected against H/D exchange, as described above. In contrast, the exchange reaction of most residues in the immature fibrils was found to be more rapid. Among them, only two consecutive regions around residues L40 and F62 were prominent. While residues belonging to these two regions were protected to a similar extent as those in mature fibrils, the other residues were subjected to rapid exchange with only 10–40% of the initial intensity retained after 11.5 h.

To analyze the exchange kinetics, the peak ratios given in Fig. 5 were plotted against exchange time (Fig. 6A). Although these plots should represent a single exponential decay as usually observed in the case of monomeric proteins, large deviations were found in many residues in the fibrils. Even if the plot could be fitted to a single exponential function, the fitted curve did not decay to zero and instead approached a plateau corresponding to the relative remaining amplitude (A_∞), which was much larger than zero. Thus, most residues were characterized by a relatively rapid decrease in intensity followed by a very slow phase represented by an almost flat line in the time range examined. We
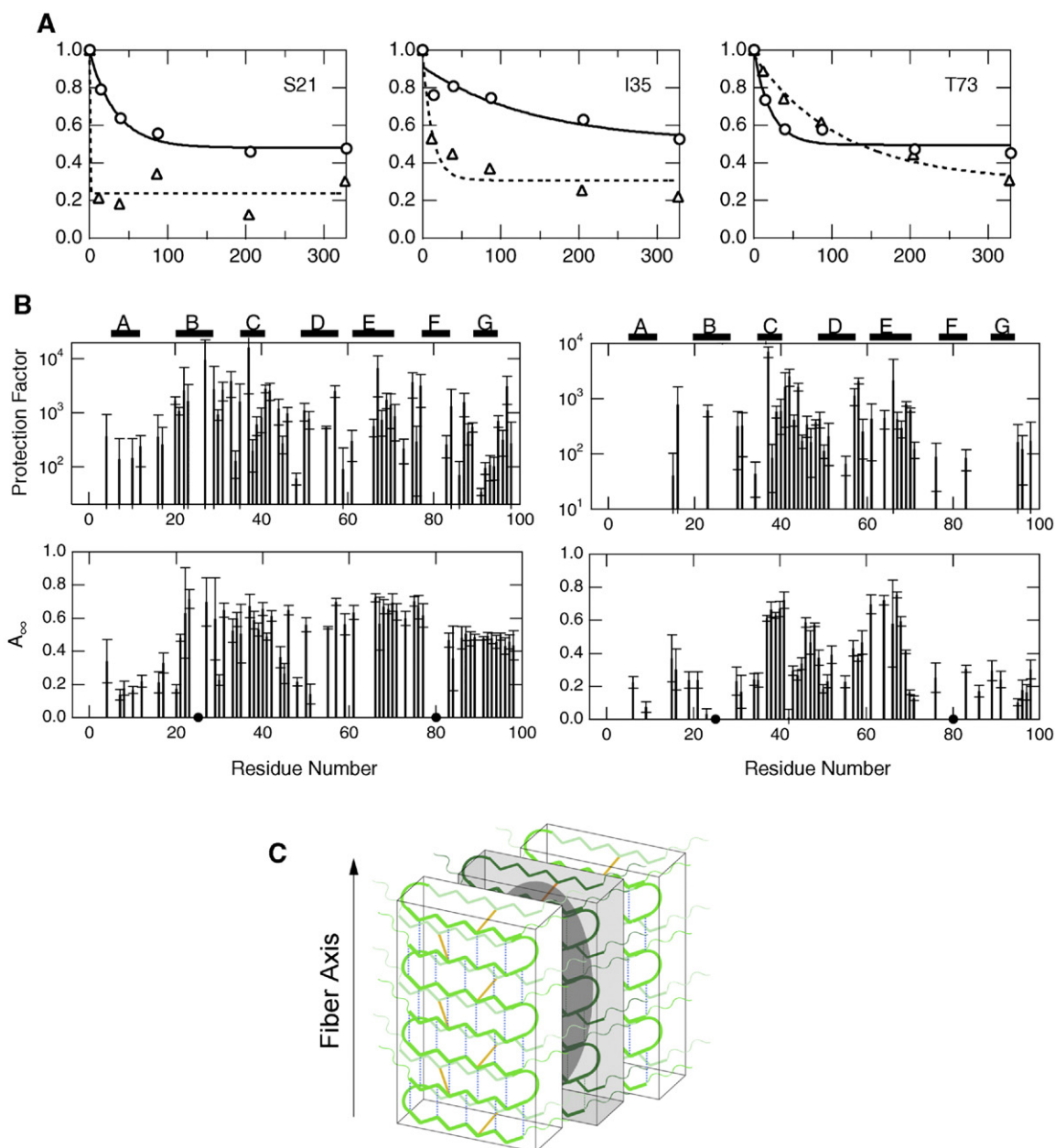

Fig. 6. (A) The exchange kinetics of mature (circles) and immature (triangles) fibrils for representative residues. The results of Ser21 (left), Ile35 (middle), and Thr73 (right) are shown. Lines between data points represent fitted curves to single exponential functions. (B) Protection factor (top) and the amplitude at time infinity (A_∞, bottom) of mature (left) and immature (right) amyloid fibrils of β2-m. (C) Schematic model of amyloid fibrils, which is consistent with the biphasic H/D exchange kinetics. Amyloid fibrils are formed with several pieces of protofilament. Outer sides of protofilaments, shown in light color, can be exchanged relatively easily, while the inner sides of the protofilaments, shown in dark color, are not subject to H/D exchange. The figure was taken from Yamaguchi et al. [4] with permission.

consider that this biphasic behavior of the exchange kinetics in amyloid fibrils could be explained by taking account the fact that the amyloid fibrils are large molecular assemblies composed of huge numbers of protein molecules, and each protein molecule could be structurally different from each other in the context of burial and shielding from solvent molecules (see below).

Based on the two-component mechanism, in which one exchanges by first-order kinetics with k_{ex} and the other is represented by A_∞, which does not exchange in the time range examined, we further characterized the exchange kinetics of amyloid fibrils. To take into account the sequence effect, we converted k_{ex} into a protection factor (P). Considering that the exchange reaction proceeded at pD 2.5, where the intrinsic rate constant is at a minimum for most amino acids, the EX2 conditions ($k_c >> k_{int}$) are reasonably fulfilled. As shown in Fig. 6B, the plots of the protection factors against residue numbers for mature and immature fibrils, as well as the remaining amplitude (A_∞) again focus on the contrasting patterns between the two types of fibrils.

In the case of mature fibrils, the protection factors of most residues were uniform and consistent with the apparent exchange time course. Intriguingly, the profile of the remaining amplitudes resembled that of the protection factors. Thus, in terms of both parameters (P and A_∞), the N-terminal residues were relatively less protected, while most of the other residues were uniformly protected. The protection factors of these residues were in the range from 10^3 to 10^4, slightly smaller than those of the protected core of the globular proteins. Nevertheless, these values are surprisingly higher than those found in most non-native conformations of proteins, which are usually, at most, of the order of 100. This unexceptionally large value in protection factors may account for the apparent stability of amyloid fibrils often observed as protease resistance, and found in chemical and thermal denaturation [29,30].

For the immature fibrils, although the protected regions were found only in narrow regions around L40 and F62, the values of protection factors of the protected residues were as large as those in mature fibrils, indicating that the protected core regions are as rigid as those of mature fibrils. Again, the profile of the remaining amplitude is similar to that of the protection factor. The hydropathy profile plotted in Fig. 5F reveals four major hydrophobic regions along the sequence. Among them, the second and third parts coincide well with the two regions constituting the core of the immature fibrils. The absence of the first and fourth parts (A and D) from the core is a remarkable feature of the immature fibril as compared with the mature fibril. Furthermore, the core of the immature fibril is predominantly composed of hydrophobic regions, whereas that of the mature fibril contains hydrophobic and hydrophilic regions in equal proportions. This suggests that hydrophobic interactions other than hydrogen bonds between the β-strands play an important role with regard to the stability of the immature fibril. This is consistent with the view that immature fibrils are formed under high salt conditions where hydrophobic interactions are strengthened and that they are formed spontaneously without seeds implying that specific interactions such as electrostatic interaction are less important [25,28].

4.2. Amyloid-β peptide

The DMSO-quenched H/D exchange method described in this study is generally applicable to various amyloid fibrils formed by different proteins. Many reports have analyzed the structure of amyloid fibrils using basically the same technique described here, including the amyloid-like fibrils formed by human or yeast prion proteins [11,31]. Among them, the amyloid fibrils formed by amyloid-β (Aβ) peptide have been extensively studied by several groups. Whittemore et al. [32] investigated the structure of amyloid fibrils formed by Aβ(1–40) peptide. They incubated preformed amyloid fibrils of Aβ(1–40) for 25 h in deuterated buffer to perform partial H/D exchange, and then transferred the partially exchanged peptide into quenching buffer of 95% (v/v) DMSO/5% (v/v) dichloroacetate. They found that the amide hydrogen in about half of the residues was exchanged with D_2O during the incubation time of 25 h. The ratio between exchanged and reference spectra showed a specific pattern in which N- and C-terminal residues were less protected from exchange. In contrast, the residues in the middle part of the molecule ranging K16–V36 were mostly protected, suggesting that many of the residues in this region are involved in a β-structure in the fibril. The protected region in the middle part of the molecule was separated into two parts by readily exchangeable residues, G25 and S26, which may be located on a turn or a flexible part of the peptide.

The structure of the more toxic form of amyloid-β peptide, Aβ(1–42), was also investigated by the DMSO-quenching H/D exchange method [33,34]. Lührs et al. [34] applied a similar method to that described in this study to the amyloid fibril formed by Aβ(1–42). They further improved this method in several ways. Although the exchange rates greatly decrease by ~100 times in the presence of 95% (v/v) DMSO, non-negligible further exchange does still occur, as mentioned above. In order to eliminate the effect of exchange in DMSO-quenching buffer, the two-step exponential fit in which a series of HSQC spectra were recorded in DMSO-quenching buffer was fitted to obtain the extrapolated value of proton occupancy at time zero of measurement. To perform this, they measured a series of 80 HSQC spectra for 4 h (3 min per spectrum). In addition, to discriminate the residues whose exchange rate in DMSO was too rapid to be followed even by using this method, they added a mixture of 0.5 M H_2O and 0.5 M D_2O to the sample in which a series of 80 HSQC spectra had been already measured, and recorded another series of 80 HSQC spectra. They found that the peak intensities of several residues dropped to half of that before the addition of the 50% mixture of H_2O/D_2O, indicating that the intrinsic rate of these residues was too rapid to be followed. Using this method, they concluded that D1, A2, D7, H14, and A30 were excluded from the analysis. Nevertheless, most of the other residues were slow enough to be analyzed, and yielded precise exchange rates for 88% of the amino acid residues in the sequence of Aβ(1–42) and 96% of the amino acid in the core of the protofilament.

The kinetic analysis of amyloid fibrils formed by Aβ(1–42) revealed the different behaviors between residues in the N-terminal and C-terminal regions. In the residues in the N-

terminal segment (D1-L17), about half of the intensity of amide protons exchanged rapidly ($k_{ex} > 10$ h^{-1}); however, the other half exchanged very slowly ($k_{ex} < 10^{-2}$ h^{-1}). Similar biphasic behavior to β2-m discussed above was observed, and the authors attributed this biphasic behavior in the exchange kinetics to the structural heterogeneity of the Aβ(1–42) amyloid fibrils in this segment. In contrast to the N-terminal segment of the molecules, the residues in the C-terminal part exhibited no rapidly exchanging population, resulting in exclusively single exponential decay with a very slow rate constant. Within the slowly exchanging part of the molecule in the C-terminal, two consecutive groups of residues in the ranges V18–N27 and I31–I41 were revealed to be highly protected from exchange, suggesting the presence of two β-strands β1 and β2.

Based on the results of the DMSO-quenched HX, and extensive pairwise mutagenesis approach, they modeled the three-dimensional structure of amyloid fibrils of Aβ(1–42). Although N-terminal residues from D1 to L17 are disordered, residues V18 to I42 form a β-strand-turn-β-strand motif that contains two intermolecular, parallel, in-register β-sheets that are formed by V18–S26 and I31–I42.
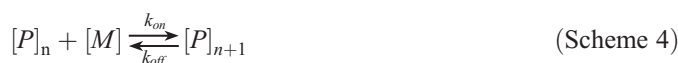
4.3. H/D exchange mechanism of amyloid fibrils

The exchange kinetics of β2-m amyloid fibrils clearly deviated from simple exponential decay in which the peak intensity at time infinity should approach zero. Although the plot could be fitted to a single exponential function with a single rate constant, the fitted curve did not decay to zero, instead it approached a plateau corresponding to the relative remaining amplitude, which was much larger than zero. Therefore, the signal decay of most residues showed at least two kinetic phases with a relatively fast exchange reaction followed by a very slow phase represented by an almost flat line. Similar biphasic behavior in the kinetics was observed in the N-terminal part of the amyloid fibrils formed by Aβ(1–40) and Aβ(1–42) [32,35].

Considering the supramolecular structure of amyloid fibrils, this biphasic behavior of the exchange kinetics can be explained as follows. In contrast to soluble globular proteins, amyloid fibrils are a supramolecular complex composed of a huge number of molecules. Although each molecule is chemically identical, the position and environment in the amyloid fibril may be different between molecules (Fig. 6B). The supramolecular organization of amyloid fibrils is considered to be composed of several protofilaments wound around one another in a left-handed manner. The protofilaments themselves consist of several layers of a cross-β-sheet structure associated with each other at a distance of 10–15 Å determined by the interaction between protruding side chains from stacked β-sheets. Therefore, there are at least two kinds of molecule in a supramolecular structure of amyloid fibrils, even though the amyloid fibrils themselves are highly homogeneous. Amino acid residues in a molecule that are located at the surface of a protofilament are expected to exchange with the solvent relatively rapidly, while those in a molecule buried inside a protofilament are considered highly resistant against exchange. In addition, lateral assembly of protofilaments into mature

amyloid fibrils would further bury part of the molecule inside the fibrils.

Another mechanism has also been proposed by Carulla et al. [36] to explain the H/D exchange in amyloid fibrils. They examined the H/D exchange reaction of amyloid fibril formed by the SH3 domain of the α-subunit of bovine phosphatidylinositol-3′-kinase. While exchange kinetics monitored by DMSO-quenched H/D exchange detected by 2D NMR showed similar biphasic behavior to β2-m and the N-terminal part of Aβ(1–42), simultaneous observation of exchange kinetics by electrospray ionization mass spectroscopy detected only two species with different molecular weights. The two species with different masses represented almost fully (apart from very labile side chain hydrogen) protonated and fully deuterated molecules.

It has been shown for various proteins that amyloid fibrils can be reconstituted in a test tube if buffer conditions are carefully selected. As the kinetic model for fibril elongation, the linear elongation model has been well established [37,38]. In this model, the denatured protein molecule binds to one end of the pre-existing amyloid fibril constituted n-mer, resulting in the formation of (n+1)-mer of the molecule.

$$[P]_n + [M] \underset{k_{off}}{\overset{k_{on}}{\rightleftharpoons}} [P]_{n+1} \qquad \text{(Scheme 4)}$$

During the H/D exchange reaction of amyloid fibrils, the elongation of amyloid fibrils apparently ceased. However, there must be a dynamic equilibration in which a molecule on the terminal(s) of the fibril detaches from the fibril, and on the other hand, a new member of the protein molecule attaches on the tip of the fibrils. Considering this dynamic recycling of molecules under equilibrium, Carulla et al. [36] proposed a molecular recycling mechanism for the H/D exchange reaction in the amyloid fibrils. In this model, while amyloid fibrils are highly protected from H/D exchange, the monomeric protein molecules dissociated from terminal(s) are susceptible to exchange. This dynamic nature is considered common in amyloid fibrils formed by other proteins.

4.4. Membrane-inserted and membrane interacting protein

The membrane inserted proteins and the membrane interacting proteins are other challenging targets for structural biology. The same reasons for amyloid fibrils are applied: The hydrophobic environment provided by the phospholipid membrane is an essential scaffold for the membrane proteins; however, the complex with phospholipid molecules has much higher molecular weight and is difficult to crystallize. Only a few examples have been found in the literature where detergent dissolved and reconstructed complexes with proteins have been crystallized, or micelle inserted forms of proteins have been determined by solution state NMR (see the references in Torres et al. [39]). Similar strategy described here can also be applied to membrane proteins to obtain valuable information on the structure and dynamics. Dempsey [40] presented a similar idea to investigate the interaction between membrane interacting protein and phospholipid membrane. He investigated the

interaction of venom toxin, melittin, with membrane micelle composed of phosphatidylcholine and phosphatidylglycerol using the partial H/D exchange followed by lyophilization and dissolution in MeOH. He found that the H/D exchange in pure methanol was suppressed slow enough to record several 2D-homonuclear spectra within several hours.

Many amyloidogenic proteins, such as amyloid-β peptide, α-synuclein, and calcitonins, are suggested to interact with biological membranes, and these interactions are considered critical steps in the formation of amyloid fibrils and diseases, as described in this special issue. Although phospholipid compositions – and therefore the physicochemical properties such as hydrophobicity and electrical charge – of biological membranes are diverse, a combination of strongly and weakly hydrophobic organic solvents, such as chloroform and DMSO, are expected to dissolve them and interacting membrane proteins to the monomeric components. Partial H/D exchange followed by dissolution/quenching by organic solvents can be successfully applied to provide valuable information on the structure, dynamics, and interaction of amyloidogenic proteins and biological membranes.

5. Concluding remarks

The DMSO-quenched H/D exchange method revealed the structure and stability of various amyloid fibrils at residue resolution. This method can be generally applied to various amyloid fibrils to provide high-resolution mapping of the hydrogen bonding network and the thermodynamic stability. Detailed analysis of the exchange kinetics revealed the nature of the supramolecular structural complex of the amyloid fibrils. Although this method, by itself, cannot determine the detailed 3D structure of the amyloid fibrils, combination with other strategies, such as the pairwise mutagenesis approach, can provides a detailed 3D model structure. The combination of this method and other complementary techniques, such as mass spectroscopy, revealed the dynamic nature of amyloid fibrils where protein molecules are dissociating and re-associating within the fibril population. Furthermore, it can be generally applied to other biological systems, and has a great potential for studying the interaction of amyloidogenic and other proteins with biological membranes.

Acknowledgments

References

[1] R. Nelson, M.R. Sawaya, M. Balbirnie, A.Ø. Madsen, C. Riekel, R. Grothe, D. Eisenberg, Structure of the cross-β spine of amyloid-like fibrils, Nature 435 (2005) 773–778.

[2] O.S. Makin, E. Atkins, P. Sikorski, J. Johansson, L.C. Serpell, Molecular basis for amyloid fibril formation and stability, Proc. Natl. Acad. Sci. U. S. A. 102 (2005) 315–320.

[3] M. Hoshino, H. Katou, Y. Hagihara, K. Hasegawa, H. Naiki, Y. Goto,

[4] K. Yamaguchi, H. Katou, M. Hoshino, K. Hasegawa, H. Naiki, Y. Goto, Core and heterogeneity of β₂-microglobulin amyloid fibrils as revealed by H/D exchange, J. Mol. Biol. 338 (2004) 559–571.

[5] Y. Bai, T.R. Sosnick, L. Mayne, S.W. Englander, Protein folding intermediates: native-state hydrogen exchange, Science 269 (1995) 192–197.

[6] V. Forge, M. Hoshino, K. Kuwata, M. Arai, K. Kuwajima, Y. Goto, Is folding of β-lactoglobulin non hierarchic? Intermediate with native-like β-sheet and non-native α-helix, J. Mol. Biol. 296 (2000) 1039–1051.

[7] H. Katou, M. Hoshino, H. Kamikubo, C.A. Batt, Y. Goto, Native-like β-hairpin retained in the cold-denatured state of bovine β-lactoglobulin, J. Mol. Biol. 310 (2001) 471–484.

[8] K. Kuwata, R. Shastry, H. Cheng, M. Hoshino, C.A. Batt, Y. Goto, H. Roder, Structural and kinetic characterization of early folding events in β-lactoglobulin, Nat. Struct. Biol. 8 (2001) 151–155.

[9] N. Hirota-Nakaoka, K. Hasegawa, H. Naiki, Y. Goto, Dissolution of β₂-microglobulin amyloid fibrils by dimethylsulfoxide, J. Biochem. 134 (2003) 159–164.

[10] A. Alexandrescu, An NMR-based quenched hydrogen exchange investigation of model amyloid fibrils formed by cold shock protein A, Pac. Sump. Biocomput. (2001) 67–78.

[11] K. Kuwata, T. Matumoto, H. Cheng, K. Nagayama, T.L. James, H. Roder, NMR-detected hydrogen exchange and molecular dynamics simulations provide structural insight into fibril formation of prion protein fragment 106–126, Proc. Natl. Acad. Sci. U. S. A. 100 (2003) 14790–14795.

[12] Y. Bai, J.S. Milne, L. Mayne, S.W. Englander, Primary structure effects on peptide group hydrogen exchange, Proteins Struct. Funct. Genet. 17 (1993) 75–86.

[13] S.W. Englander, N.R. Kallenbach, Hydrogen exchange and structural dynamics of proteins and nucleic acids, Q. Rev. Biophys. 16 (1983) 521–655.

[14] C. Woodward, I. Simon, E. Tüchsen, Hydrogen exchange and dynamic structure of proteins, Mol. Cell. Biochem. 48 (1982) 135–160.

[15] Y.Z. Zhang, Y. Paterson, H. Roder, Rapid amide proton exchange rates in peptides and proteins measured by solvent quenching and two-dimensional NMR, Protein Sci. 4 (1995) 804–814.

[16] P.J. Bjorkman, M.A. Saper, B. Samraoui, W.S. Bennett, J.L. Strominger, D.C. Wiley, Structure of the human class-I histocompatibility antigen, Hla-A2, Nature 329 (1987) 506–512.

[17] F. Gejyo, T. Yamada, S. Odani, Y. Nakagawa, M. Arakawa, T. Kunitomo, H. Kataoka, M. Suzuki, Y. Hirasawa, T. Shirahama, A.S. Cohen, K. Schmid, A new form of amyloid protein associated with chronic hemodialysis was identified as β₂-microglobulin, Biochem. Biophys. Res. Commun. 129 (1985) 701–706.

[18] S. Jones, D.P. Smith, S.E. Radford, Role of the N and C-terminal strands of β₂-microglobulin in amyloid formation at neutral pH, J. Mol. Biol. 330 (2003) 935–941.

[19] N.M. Kad, S.L. Myers, D.P. Smith, D.A. Smith, S.E. Radford, N.H. Thomson, Hierarchical assembly of β₂-microglobulin amyloid *in vitro* revealed by atomic force microscopy, J. Mol. Biol. 330 (2003) 785–797.

[20] M. Monti, S. Principe, S. Giorgetti, P. Mangione, G. Merlini, A. Clark, V. Bellotti, A. Amoresano, P. Pucci, Topological investigation of amyloid fibrils obtained from β₂-microglobulin, Protein Sci. 11 (2002) 2362–2369.

[21] T. Chiba, Y. Hogihara, T. Higurashi, K. Hasegawa, H. Naiki, Y. Goto, Amyloid fibril formation in the context of full-length protein, J. Biol. Chem. 278 (2003) 47016–47024.

[22] S. Yamamoto, K. Hasegawa, I. Yamaguchi, S. Tsutsumi, J. Kardos, Y. Goto, F. Gejyo, H. Naiki, Low concentrations of sodium dodecyl sulfate induce the extension of β₂-microglobulin-related amyloid fibrils at a neutral pH, Biochemistry 43 (2004) 11075–11082.

[23] Y. Ohhashi, Y. Hagihara, G. Kozhukh, M. Hoshino, K. Hasegawa, I. Yamaguchi, H. Naiki, Y. Goto, The intrachain disulfide bond of β₂-microglobulin is not essential for the immunoglobulin fold at neutral pH, but is essential for amyloid fibril formation at acidic pH, 131 J. Biochem. 45–52.

[24] I. Yamaguchi, K. Hasegawa, H. Naiki, T. Mitsu, Y. Matuo, F. Gejyo,

Mapping the core of the β₂-microglobulin amyloid fibril by H/D exchange, Nat. Struct. Biol. 9 (2002) 332–336.

Extension of A β_2M amyloid fibrils with recombinant human β_2-microglobulin, Amyloid 8 (2001) 30–40.

[25] D.P. Hong, M. Gozu, K. Hasegawa, H. Naiki, Y. Goto, Conformation of β_2-microglobulin amyloid fibrils analyzed by reduction of the disulfide bond, J. Biol. Chem. 277 (2002) 21554–21560.

[26] H. Katou, T. Kanno, M. Hoshino, Y. Hagihara, H. Tanaka, T. Kawai, K. Hasegawa, H. Naiki, Y. Goto, The role of disulfide bond in the amyloidogenic state of β_2-microglobulin studied by heteronuclear NMR, Protein Sci. 11 (2002) 2218–2229.

[27] N.M. Kad, N.H. Thomson, D.P. Smith, D.A. Smith, S.E. Radford, β_2-microglobulin and its deamidated variant, N17D form amyloid fibrils with a range of morphologies in vitro, J. Mol. Biol. 313 (2001) 559–571.

[28] V.J. McParland, N.M. Kad, A.P. Kalverda, A. Brown, P. Kirwin-Jones, M.G. Hunter, M. Sunde, S.E. Radford, Partially unfolded states of β_2-microglobulin and amyloid formation in vitro, Biochemistry 39 (2000) 8735–8746.

[29] T. Narimoto, K. Sakurai, A. Okamoto, E. Chatani, M. Hoshino, K. Hasegawa, H. Naiki, Y. Goto, Conformational stability of amyloid fibrils of β_2-microglobulin probed by guanidine-hydrochloride-induced unfolding, FEBS Lett. 576 (2004) 313–319.

[30] K. Sasahara, H. Naiki, Y. Goto, Kinetically controlled thermal response of β_2-microlobulin amyloid fibrils, J. Mol. Biol. 352 (2005) 700–711.

[31] C. Ritter, M.L. Maddelein, A.B. Siemer, T. Luhrs, M. Ernst, B.H. Meier, S. J. Saupe, R. Riek, Correlation of structural elements and infectivity of the HET-s prion, Nature 435 (2005) 844–848.

[32] N.A. Whittemore, R. Mishra, I. Kheterpal, A.D. Williams, R. Wetzel, E.H. Serpersu, Hydrogen-deuterium (H/D) exchange mapping of $A\beta_{1-40}$ amyloid fibril secondary structure using nuclear magnetic resonance spectroscopy, Biochemistry 44 (2005) 4434–4441.

[33] A. Olofsson, E. Sauer-Eriksson, A. Öhman, The solvent protection of amyloid-β-(1–42) fibrils as determined by solution NMR spectroscopy, J. Biol. Chem. 281 (2006) 477–483.

[34] T. Lührs, C. Ritter, M. Adrian, D. Riek-Loher, B. Bohrmann, H. Döbeli, D. Schubert, R. Riek, 3D structure of Alzheimer's amyloid-β(1–42) fibrils, Proc. Natl. Acad. Sci. U. S. A. 102 (2005) 17342–17347.

[35] I. Kheterpal, A. Williams, C. Murphy, B. Bledsoe, R. Wetzel, Structural features of the Aβ amyloid fibril elucidated by limited proteolysis, Biochemistry 40 (2001) 11757–11767.

[36] N. Carulla, G.L. Caddy, D.R. Hall, J. Zurdo, M. Gairí, M. Feliz, E. Giralt, C.V. Robinson, C.M. Dobson, Molecular recycling within amyloid fibrils, Nature 436 (2005) 554–558.

[37] H. Naiki, F. Gejyo, Kinetic analysis of amyloid fibril formation, Methods Enzymol. 309 (1999) 305–318.

[38] H. Naiki, N. Hashimoto, S. Suzuki, H. Kimura, K. Nakakuki, F. Gejyo, Establishment of a kinetic model of dialysis-related amyloid fibril extension in vitro, Amyloid 4 (1997) 223–232.

[39] J. Torres, T.J. Stevens, M. Samsó, Membrane proteins: the 'Wild West' of structural biology, Trends Biochem. Sci. 28 (2003) 137–144.

[40] C.E. Dempsey, Amide-resolved hydrogen–deuterium exchange measurements from membrane-reconstituted polypeptides using exchange trapping and semiselective two-dimensional NMR, J. Biomol. NMR 4 (1994) 879–884.

[41] J. Kyte, R.F. Doolittle, A simple method for displaying the hydrophobic character of a protein, J. Mol. Biol. 157 (1982) 105–132.